

During running in place, grid cells integrate elapsed time and distance run

Benjamin J. Kraus, Mark P. Brandon, Robert J. Robinson II, Michael A. Connerney,
Michael E. Hasselmo, Howard Eichenbaum

Supplemental Information

Movie S1: Firing activity of grid cell during treadmill running, related to Figure 1.

Three complete runs on the treadmill embedded in the stem of the figure-eight maze (Figure 1A). One red (back) and one green (front) LED are mounted on the microdrive and used to track the rat's position. The firing activity of one neuron is indicated by both a blinking magenta dot that follows the location of the rat, as well as an audible clicking noise. This neuron is the same neuron shown in Figure 1D. A red triangle appears in the upper left corner when the treadmill is active.

Figure S1

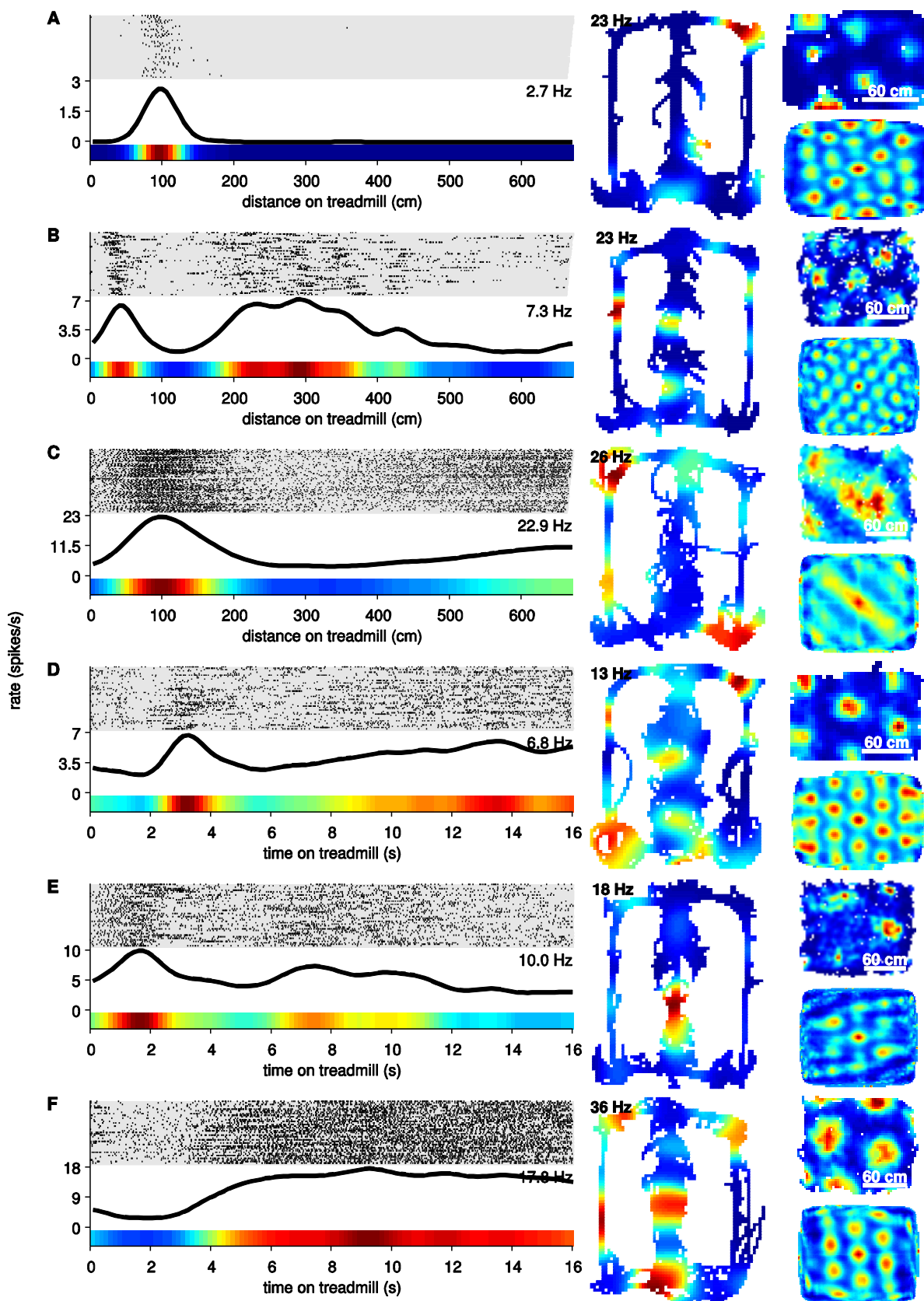


Figure S1: Grid cells fire at specific times and distances during treadmill running (additional examples), related to Figure 1 and Movie S1.

Additional example grid cells showing their firing patterns during treadmill running, maze running, and open field foraging. For each example grid cell, the left column shows firing patterns during treadmill running in raster plots (left-top), histograms of average firing over time (left-middle), and normalized firing rate plots (left-bottom). The middle column shows spatial firing patterns during maze traversal (when the treadmill is stopped). Number in the upper-left corner indicates peak firing rate on the maze. The right column shows open field spatial firing patterns (right-top) and spatial autocorrelations (right-bottom). In distance-fixed sessions (top three examples), activity is plotted in terms of distance run during treadmill runs; in time-fixed sessions (bottom three examples), activity is plotted in terms of elapsed time. See also Figure 1 and Movie S1.

Figure S2

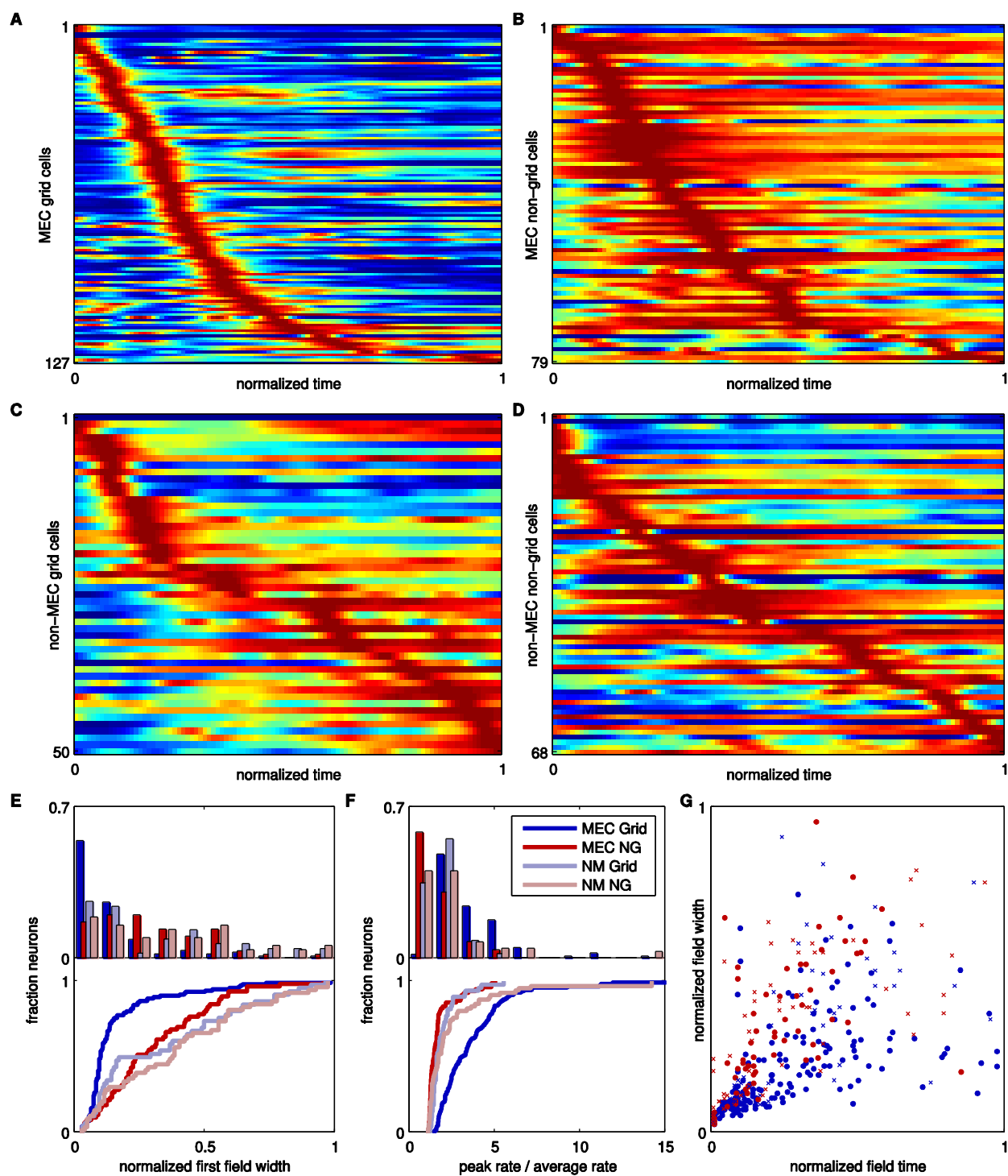


Figure S2: Grid cells during treadmill running (breakdown by region), related to Figure 2.

(A-D) Ensemble firing rate maps showing normalized spiking rate during treadmill running for grid cells recorded from the MEC (A), non-grid cells recorded from the MEC (B), grid cells recorded from outside the MEC (C), and non-grid cells recorded from outside the MEC (D).

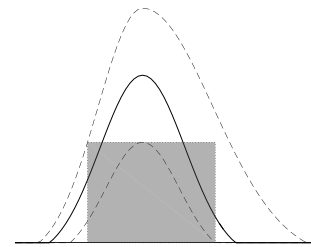
Firing rate is plotted in terms of “fraction of run” to allow ensemble analysis across both time-fixed and distance-fixed sessions. (E) Distribution (top) and cumulative distribution (bottom) of the width of the first firing field for each neuron. Firing field width was calculated using the method described in the experimental procedures and illustrated by this sketch. In the sketch:

dashed lines indicate upper and lower confidence bounds, solid line indicate the mean firing rate, width of the shaded area reflects calculated firing field

location and width, height of shaded region reflects the peak value of the lower confidence interval. Note that the left edge of

the firing field was bounded by the upper confidence bound

crossing below the peak value of the lower confidence bound,



while the right edge of the firing field was bounded by the lower confidence bound crossing

below zero. (F) Distribution (top) and cumulative distribution (bottom) of the peak rate of each neuron divided by the average rate of each neuron. A smaller value indicates broader firing

fields. Legend in panel F applies to panels E, F, and G. NM = Non-MEC, NG = Non-Grid. (G)

Distribution of field widths as a function of the time of peak firing. Solid dots are MEC cells, x's are non-MEC cells. Fields cut off by the end of the treadmill were left off for clarity. MEC grid cells showed significantly narrower firing fields (Kolmogorov–Smirnov Test: $p = 6 \times 10^{-5}$;

Wilcoxon Rank Sum Test: $p = 2 \times 10^{-5}$) and significantly sharper tuning (Kolmogorov–Smirnov Test: $p = 9 \times 10^{-22}$; Wilcoxon Rank Sum Test: $p = 4 \times 10^{-21}$) than non-MEC grid cells, despite no

differences in spatial tuning between grid cells within MEC and outside MEC (see Figure S5). See also Figures 2 and S5.

Figure S3

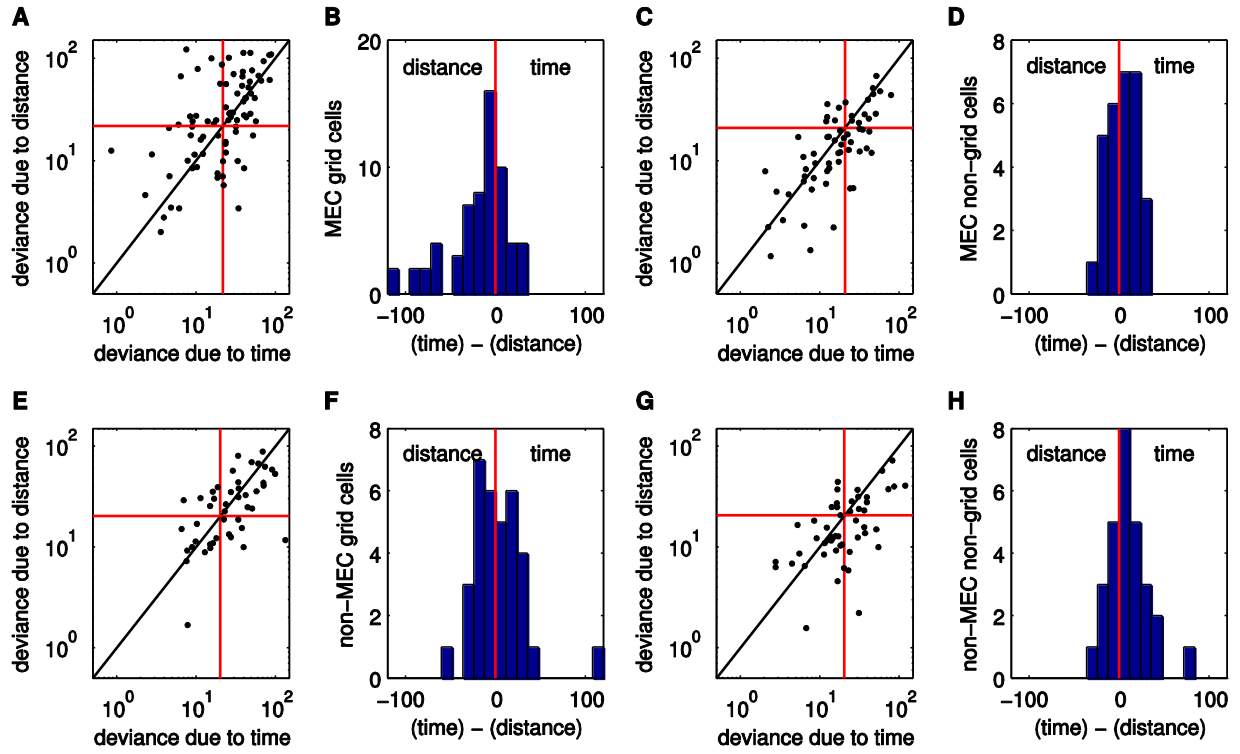


Figure S3: Grid cells encode both distance and time (breakdown by region), related to Figures 4F-4I, and Table S2.

(A, C, E, G) Deviance of two generalized linear models comparing the effect of removing time versus removing distance. The x-axis shows the deviance of the space + distance model from the full (space + distance + time) model, effectively measuring the contribution of time to the full model. The y-axis shows the deviance of the space + time model from the full (space + distance + time) model, effectively measuring the contribution of distance to the full model. Dots indicate deviances for either grid cells recorded from the MEC (A), non-grid cells recorded from the MEC (C), grid cells recorded from outside the MEC (E), and non-grid cells recorded from outside the MEC (G). Dots above the diagonal prefer distance; below the diagonal prefer time; above the horizontal red line are significantly influenced by distance; to the right of the vertical red line are significantly influenced by time. Thresholds for significance are based on a χ^2 test taking into account the number of parameters removed from each model (5 degrees of freedom), and adjusted using Bonferroni correction to account for multiple comparisons. (B, D, F, H) Strength of time versus distance coding measured as the difference between time and distance deviances for the cells shown in panels A, C, E, and G respectively. See also Figures 4F-4I and Table S2.

Figure S4

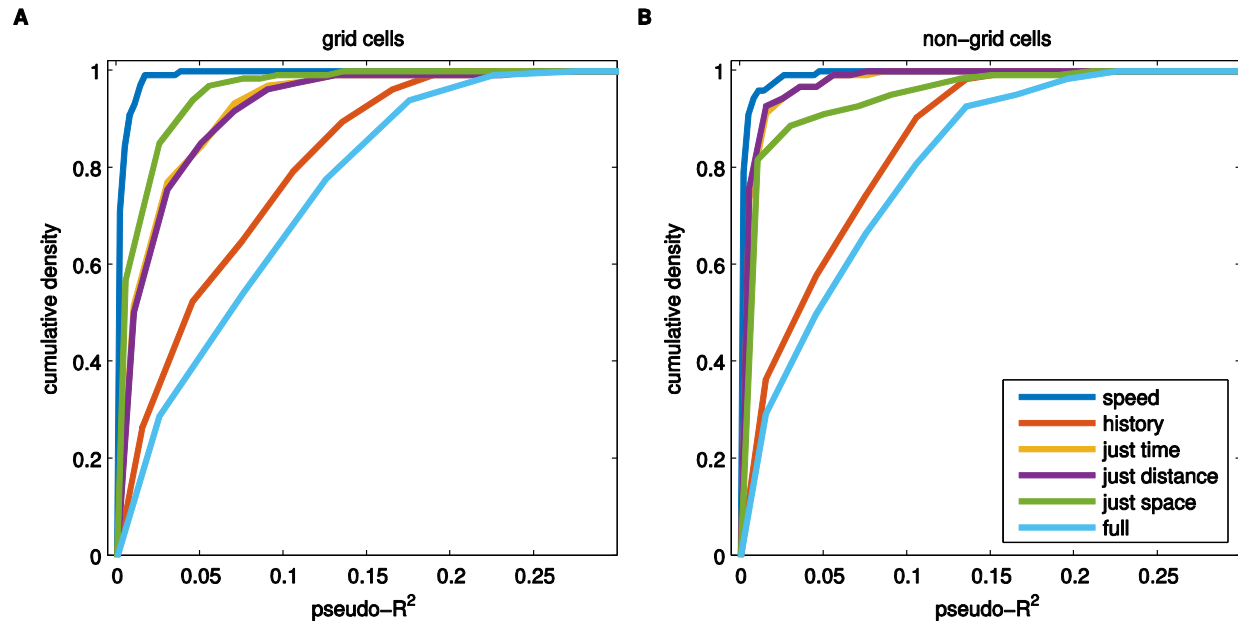


Figure S4: Pseudo-R² calculations for generalized linear models, related to Figures 4F-4I and Table S3.

Cumulative distribution of the pseudo-R² values calculated for each neuron for each of six different generalized linear models for grid cells (A) and non-grid cells (B). The “full” model is the same as the “time + distance” model used for the deviance calculations (Figures 4F-4I and Table S2), and included spike history, treadmill speed, and space as well as time and distance. “Just time”, “just distance”, and “just space” emphasize that these models included just those sets of parameters (without spiking history or speed), in contrast to the “time”, “distance” models used for deviance calculations, which included spiking history, speed, and space in order to account for the impact of these parameters on spiking rate. See also Figures 4F-4I and Tables S3 and S4.

Figure S5

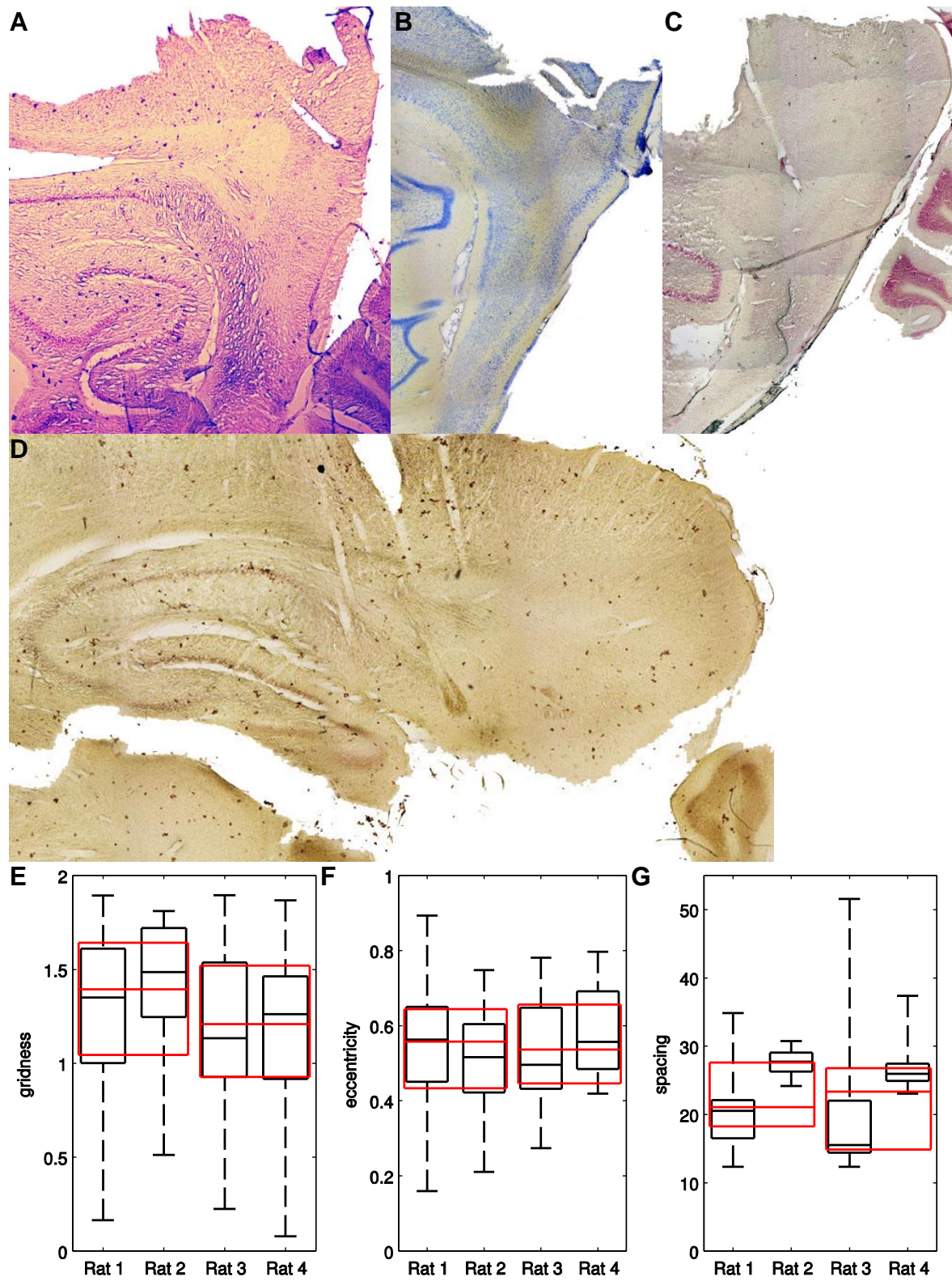


Figure S5: Representative histology and grid quality measures, related to Figures 2 and S2.

Representative Nissl-stained sagittal sections show tetrodes tracks associated with grid cell recording for each animal included in the study. (A-B) Tetrode tracks were observed in the superficial layers of the MEC in Rats 1 and 2. (C) Tetrode tracks show that grid cells from Rat 3 were recorded from the border of the deep layers of medial entorhinal cortex and parasubiculum. (D) Tetrodes from Rat 4 were found to terminate in the dorsal subiculum and dorsal presubiculum. (E-G) Box plots comparing the relative gridness (E), eccentricity (F), and spacing (G) of grid cells in each rat and by pairs of rats that compose the MEC and non-MEC groupings. Black box plots show individual rat data: The middle line indicates the median, the box extends from the 25th to 75th percentile, and the whiskers show the full extent of the data for each rat. Red boxes show group data for MEC and non-MEC groupings, indicating median, 25th, and 75th percentiles. The gridness, eccentricity, and spacing are calculated based on the six peaks in the autocorrelation identified by the gridness algorithm described in the Experimental Procedures. The eccentricity ranges from 0 to 1 and is a measure of how close the six peaks fit a circle (eccentricity of 0 is a perfect circle). The spacing is the mean distance of the six peaks from the center of the autocorrelation. Gridness scores (E) did not differ between grid cells recorded from MEC versus outside MEC (Kolmogorov–Smirnov Test: $p = 0.15$; Wilcoxon Rank Sum Test: $p = 0.06$) or among individual rats (Kruskal-Wallis ANOVA: $p = 0.19$). Eccentricity (F) also did not differ between grid cells recorded from MEC versus outside MEC (Kolmogorov–Smirnov Test: $p = 0.73$; Wilcoxon Rank Sum Test: $p = 0.36$) or among individual rats (Kruskal-Wallis ANOVA: $p = 0.40$). Grid field spacing (G) also did not differ between grid cells recorded from MEC versus outside MEC (Kolmogorov–Smirnov Test: $p = 0.31$; Wilcoxon Rank Sum Test: $p = 0.29$) but did significantly differ among individual rats (Kruskal-Wallis ANOVA: $p = 6 \times 10^{-10}$). In particular: Rat 1 (MEC) and Rat 3 (non-MEC) have the same spacing, Rat 2 (MEC) and Rat 4 (non-MEC) have the same spacing. These findings are consistent with previous reports of

variation in grid field spacing at distinct loci in MEC (Brun et al., 2008; Stensola et al., 2012).

These findings indicate that grid cells from within and outside MEC have the same spatial firing characteristics. See also Figures 2 and S2.

Table S1

	Rat 1	Rat 2	Rat 3	Rat 4	all
All Grid Cells	101	26	31	19	177
0 Fields	11	0	2	2	15
1 Field	49	5	20	11	85
2+ Fields	41	21	9	6	77
Non-Grid Cells	67	12	53	15	147
0 Fields	18	1	12	3	34
1 Field	39	7	32	8	86
2+ Fields	10	4	9	4	27

Table S1: Number of firing fields observed during treadmill running, related to Figure 2C.

Breakdown of the number of firing fields observed for each rat for both grid cells (top half of the table) and non-grid cells (bottom half of the table). See also Figure 2C.

Table S2

	neither	time	t > d	d > t	distance	all
Grid Cells	60	14	23	43	22	162
Rat 1	45	4	3	23	15	90
Rat 2	3	5	8	9	1	26
Rat 3	9	3	7	6	4	29
Rat 4	3	2	5	5	2	17
Non-Grid Cells	55	19	18	9	12	113
Rat 1	24	7	7	5	6	49
Rat 2	7	2	1	1	0	11
Rat 3	20	8	5	3	5	41
Rat 4	4	2	5	0	1	12
All	115	33	41	52	34	275

Table S2: Generalized linear model results, related to Figures 4F-4I.

Breakdown of the influence of time and/or distance on the firing of all grid cells (top half of table) and non-grid cells (bottom half of table) that exhibited at least one firing field during treadmill running. “Neither” indicates cells were not significantly influenced by either time or distance. “time” or “distance” indicates the cells were significantly influenced by only time or distance, but not both. “t > d” and “d > t” indicates the cells were significantly influenced by both time and distance. “t > d” indicates a stronger influence from time while “d > t” indicates a stronger influence from distance. Thresholds for significance were adjusted using Bonferroni correction to account for multiple comparisons. See also Figures 4F-4I and S3.

Table S3

	Avg. Grid Cells	Median Grid Cells	Avg. Non-Grid Cells	Median Non-Grid Cells
Full Model	0.09657	0.08920	0.06923	0.05978
Just Time	0.02938	0.01958	0.00846	0.00436
Just Distance	0.03084	0.01934	0.00819	0.00408
Just Space	0.01539	0.00757	0.01683	0.00453
History	0.07123	0.05552	0.05516	0.05097
Speed	0.00308	0.00118	0.00278	0.00102

Table S3: Pseudo-R² calculations for generalized linear models, related to Figures 4F-4I and S4, and Table S2.

Average and median pseudo-R² values for each of six different generalized linear models. “Just time”, “just distance”, and “just space” emphasize that these models included just those sets of parameters (without spiking history or speed), while the “Time”, “Distance” and “Time + Distance” models used for deviance calculations (Figures 4F-4I, and Table S2) all included spiking history, speed, and space. See also Figure S4 and Table S4.

Table S4

	Full Model	Just Time	Just Distance	Just Space	History	Speed
Figure 1B	0.1503	0.08025	0.08213	0.02269	0.0800	0.001498
Figure 1C	0.162	0.01668	0.01778	0.01016	0.1512	0.000345
Figure 1D	0.2235	0.07581	0.09816	0.00471	0.1808	0.000178
Figure 1E	0.2176	0.09851	0.09456	0.00419	0.1625	0.015554
Figure 1F	0.1888	0.07897	0.07901	0.03603	0.147	0.013016
Figure 1G	0.1191	0.02457	0.03314	0.00664	0.0964	0.000745
Figure 1H	0.1579	0.00999	0.01417	0.00271	0.146	0.000727
Figure 4A	0.2235	0.07581	0.09816	0.00471	0.1808	0.000178
Figure 4B	0.159	0.09611	0.10813	0.03408	0.068	0.001179
Figure 4C	0.0667	0.01968	0.02318	0.00694	0.0555	0.000438
Figure 4D	0.0783	0.05029	0.04956	0.02194	0.029	0.002149
Figure 4E	0.1287	0.05559	0.04461	0.03893	0.0973	0.019369
Figure S1A	0.2951	0.23529	0.24409	0.0476	0.0967	0.000245
Figure S1B	0.1191	0.02191	0.02445	0.0200	0.1055	0.000714
Figure S1C	0.0549	0.03511	0.0363	0.00443	0.0384	0.003317
Figure S1D	0.0426	0.00387	0.00451	0.00226	0.039	0.001188
Figure S1E	0.0381	0.00883	0.00864	0.00836	0.0262	0.000132
Figure S1F	0.0423	0.02135	0.02100	0.00105	0.0261	0.001071

Table S4: Pseudo-R² values for example cells, related to Figures 1, 4A-E, and S1 and Table S3.

Pseudo-R² values for six different generalized linear models for each example cell in Figures 1, 4A-4E, and S1. “Just time”, “just distance”, and “just space” emphasize that these models included just those sets of parameters (without history or speed). See also Table S3.